Contributions to Geophysics and Geodesy Vol. 44/4, 2014 (293–312)

Hydromagnetic dynamos in rotating spherical fluid shells in dependence on the Prandtl number, density stratification and electromagnetic boundary conditions

Tomáš ŠOLTIS[1], Ján ŠIMKANIN[2]

[1] Geophysical Institute, Slovak Academy of Sciences
Dúbravská cesta 9, 845 28 Bratislava, Slovak Republic
e-mail: geoftoso@savba.sk

[2] Institute of Geophysics, Academy of Sciences of the Czech Republic
Boční II/1401, 141 31 Prague, Czech Republic
e-mail: jano@ig.cas.cz

Abstract: We present an investigation of dynamo in a simultaneous dependence on the non-uniform stratification, electrical conductivity of the inner core and the Prandtl number. Computations are performed using the MAG dynamo code. In all the investigated cases, the generated magnetic fields are dipolar. Our results show that the dynamos, especially magnetic field structures, are independent in our investigated cases on the electrical conductivity of the inner core. This is in agreement with results obtained in previous analyses. The influence of non-uniform stratification is for our parameters weak, which is understandable because most of the shell is unstably stratified, and the stably stratified region is only a thin layer near the CMB. The teleconvection is not observed in our study. However, the influence of the Prandtl number is strong. The generated magnetic fields do not become weak in the polar regions because the magnetic field inside the tangent cylinder is always regenerated due to the weak magnetic diffusion.

Key words: Hydromagnetic dynamo, Non-uniform stratification, Prandtl number, Penetrative convection, Electromagnetic boundary conditions

1. Introduction

The dynamo theory, which is a significant part of cosmic magnetohydrodynamics, explains the generation mechanism and origin of the Earth's and planetary magnetic fields and their spatial and temporal evolution and

doi: 10.1515/congeo-2015-0007

changes (e.g. *Roberts and Glatzmaier, 2000; Glatzmaier, 2005; Fearn, 2007; Christensen and Wicht, 2007; Sakuraba and Roberts, 2009*). Numerical modelling of self-consistent dynamos has made noticeable progress in the last years due to the progress in computer technology. The results of numerical simulations are in very good agreement with the observations of the recent geomagnetic field and with paleomagnetic research (*Roberts and Glatzmaier, 2000; Glatzmaier, 2005; Fearn, 2007; Christensen and Wicht, 2007; Wicht and Tilgner, 2010; Sakuraba and Roberts, 2009*). Complicated processes going on in the Earth's and planetary fluid interiors, e.g., a chemical homogenisation, gravitational differentiation, solidification processes acting on the inner core boundary constitute the driving mechanism of dynamos, i.e. they are the fundamental source of convection or magnetoconvection (*Jones, 2000; Roberts and Glatzmaier, 2000; Trümper et al., 2012*). Non-uniform stratifications of the outer liquid Earth's core and the liquid interiors of Giant planets are a consequence of these processes (this means density stratification, see *Fearn and Loper, 1981; Zhang and Schubert, 2000; Stanley and Mohammadi, 2008; Bassom et al., 2011; Gubbins and Davies, 2013*).

In general, it is assumed that the upper part of the outer liquid Earth's core (close to the core-mantle boundary – CMB) is stably stratified (subadiabatic radial temperature gradient) and the lower part (towards the inner core boundary – ICB) unstably stratified (superadiabatic radial temperature gradient). The idea of "a stably stratified ocean" at the top of the outer Earth's core was firstly introduced by *Braginsky (1964)*. Models of a non-uniformly stratified fluid shell are an acceptable simplification of the real Earth-like conditions. In the Earth's core the stably stratified sublayer is probably very thin (the outer Earth's core is almost unstably stratified, see *Braginsky, 1964; Fearn and Loper, 1981; Zhang and Schubert, 2000; Šimkanin et al., 2003; Šimkanin et al., 2006; Šimkanin et al., 2010; Šimkanin et al., 2011; Stanley and Mohammadi, 2008; Bassom et al., 2011; Gubbins and Davies, 2013*). Such a stratification is probably typical for the terrestrial planets (*Zhang and Schubert, 2000; Stanley and Bloxham, 2006; Stanley and Mohammadi, 2008; Bassom et al., 2011; Gubbins and Davies, 2013*). However, in the other planets the ratio of the thickness of the appropriate sublayers (e.g., of the stably stratified to unstably stratified sublayers) and their geometric configuration vary. This is notice-

able especially with the Giant planets (*Stanley and Bloxham, 2004; Stanley and Bloxham, 2006; Zhang and Schubert, 2000; Stanley and Mohammadi, 2008*). Some examples, where the geometric configuration plays an important role, follow. Mercury is characterized by a weak magnetic field. A possible explanation could be given by a hydromagnetic dynamo working in the similar geometric configuration as supposed for the terrestrial planets (stable/unstable) but in this case a larger fraction of spherical shell is stably stratified (*Christensen, 2006*). In such a case the dynamo runs in the small unstably stratified sublayer (close to ICB). Such a weak dynamo action and skin-effect (the magnetic field generated in the unstably stratified sublayer permeates through the stably stratified sublayer where it is damped due to skin-effect) lead to the weak magnetic field observed on the surface of Mercury (*Christensen, 2006; Christensen and Wicht, 2008*). For a different geometric configuration the influence of a non-uniform stratification is fundamental. Stanley and Bloxham (*2004, 2006*) assumed reverse stratification, i.e. the stably stratified sublayer is surrounded by the unstably stratified one. This configuration leads to non-dipolar and non-axisymmetric magnetic fields, which are typical e.g., for Uranus and Neptune (*Stanley and Bloxham, 2004; Stanley and Bloxham, 2006*).

Non-uniform stratification can be simulated thermodynamically also in the Boussinesq models by means of internal heat sources (*Zhang and Schubert, 2000; Šimkanin et al., 2003; Šimkanin et al., 2006; Šimkanin et al., 2010; Šimkanin et al., 2011; Šimkanin and Hejda, 2011*). If the stably stratified sublayer is very thin (for a geometric configuration stable/unstable), then behaviour is close to the case of uniform stratification when the whole layer is unstably stratified. Likewise, if the unstably stratified sublayer is very thin, then behaviour is close to the case of uniform stratification when the whole layer is stably stratified. Thus, the effects of non-uniform stratification are noticeable when the thicknesses of the stably and unstably stratified sublayers are comparable (*Zhang and Schubert, 2000; Šimkanin et al., 2003; Šimkanin et al., 2006; Šimkanin et al., 2010; Šimkanin et al., 2011*). The simultaneous influence of the non-uniform stratification and viscous, thermal and magnetic diffusive processes on the dynamo action was investigated in *Šimkanin and Hejda (2011).* They considered a model, in which 10% of the shell is stably stratified (the upper sub-shell is stably stratified) and 90% unstably (the lower sub-shell is unstably stratified). Vis-

cous, thermal and magnetic diffusive processes constitute the second main factor which influences the dynamo. For the outer Earth's core it is expected that the kinematic viscosity $\nu = 10^{-6}\,\mathrm{m^2 s^{-1}}$, the thermal diffusivity $\kappa = 5 \times 10^{-6}\,\mathrm{m^2 s^{-1}}$ and the magnetic diffusivity $\eta = 2\,\mathrm{m^2 s^{-1}}$ (*Fearn, 2007*). Let us discuss kinematic viscosity and the thermal diffusivity, particularly the ratio ν/κ (known as the Prandtl number). In most numerical simulations scientists set $\nu/\kappa = 1$, but for the Earth's core $\nu/\kappa = 0.2$ (*Fearn, 2007*). (It is necessary to remark that some authors indicate $\nu/\kappa = 0.1 - 1$, see, e.g., *Christensen and Wicht, 2007*). The Prandtl number is the only parameter whose geophysical value can be directly used in dynamo models. *Šimkanin and Hejda (2011)* decided to set $\nu/\kappa = 0.2$ and also 1. Their results showed that the influence of non-uniform stratification is weak for their parameters, but the influence of the Prandtl number is strong (a strong dependence of hydromagnetic dynamos on the Prandtl number has been shown also in *Busse and Simitev, 2005*). They found that the magnetic field only becomes weak in the polar regions at low Prandtl numbers, when the inertia becomes important. This is a basic condition. However, whether the magnetic field is weak in the polar regions or not depends also on the magnetic diffusion. If the magnetic diffusion is small, then this phenomenon does not exist. However, if it is large, it exists because the strong magnetic diffusion significantly weakens the magnetic field inside the tangent cylinder. The magnetic diffusion and inertia seem to act in the same direction as to weaken the magnetic field inside the tangent cylinder (*Šimkanin and Hejda, 2011*).

Influence of the electrical conductivity of the inner core on hydromagnetic dynamos seems to be another interesting problem. *Roberts and Glatzmaier (2000)* and *Glatzmaier (2005)* concluded that different magnetic diffusion time scales of inner and outer cores could be responsible for the stochastic character of geomagnetic polarity reversals (on the contrary to the solar dynamo, which reverses periodically). However, *Wicht (2002)* concluded that the influence of the inner-core conductivity on Earth-like reversal sequences is insignificant for the dynamo model in his study. He showed that the influence of the inner-core conductivity on the field structure in the outer core is only marginal and the inner-core conductivity reduces the number of short dipole-polarity intervals with a typical length of a few thousand years (*Wicht, 2002*). This does not support the scenario proposed by *Roberts and*

Glatzmaier (*2000*) and *Glatzmaier (2005)*. On the other hand, *Dharmaraj and Stanley (2012)* concluded that the dynamo generation mechanism and reversal frequency are strongly dependent on the inner core conductivity. They showed that a conducting inner core can reduce the reversal frequency and that a strong planetary magnetic field intensity does not imply that the dynamo operates in the strong field regime as is usually presumed. They also showed that the combination of thermal boundary conditions and the Rayleigh number plays an important role in determining the influence of the inner core's conductivity on planetary dynamos (*Dharmaraj and Stanley, 2012*). Their results support the scenario proposed by *Roberts and Glatzmaier* (*2000*) and *Glatzmaier (2005)*. Thus, the role of inner core conductivity for reversal rate and certainly for geodynamo is still controversial.

In the present paper, we focus on the study of the simultaneous influence of the non-uniform stratification, electrical conductivity of the inner core and diffusive processes on the dynamo action. A model, in which 5% of the shell is stably stratified (the upper sub-shell is stably stratified) and 95% unstably (the lower sub-shell is unstably stratified) is considered. It is possible to discuss whether 5% is adequate for the Earth's core, whether 1% or 8% would not be a better alternative. We choose 5% because this value is still an adequate simplification for the Earth's core and we wish to analyse a difference between the cases 5% and 10% (provided in *Šimkanin and Hejda, 2011*). To study an influence of electrical conductivity of the inner core, we consider the inner core to be in the first investigated case electrically insulating, while in the second case it is electrically conducting (electrical conductivity of the outer and inner core is considered to be the same). Lastly, we set $\nu/\kappa = 0.2$, 1 and 5 to investigate an influence of viscous and thermal diffusive processes. Magnetic ones are not under study. The model and governing equations are presented in Section 2, and numerical results in Section 3. Section 4 is devoted to conclusions.

2. Governing equations and model

Here we consider dynamo action due to thermal convection of an electrically conducting incompressible fluid in the Boussinesq approximation in a non-uniformly stratified spherical shell ($r_i < r < r_o$) rotating with angular

velocity Ω. Evolution of the magnetic field $\mathbf{B}$, the velocity $\mathbf{V}$ and the temperature T is described by the system of dimensionless equations:

$$E\left(\frac{\partial \mathbf{V}}{\partial t}+(\mathbf{V}\cdot\nabla)\,\mathbf{V}-\nabla^2\mathbf{V}\right)+2\mathbf{1}_z\times\mathbf{V}+\nabla P= \\ =R_a\frac{\mathbf{r}}{r_o}T+\frac{1}{P_m}(\nabla\times\mathbf{B})\times\mathbf{B}\,, \qquad (1)$$

$$\frac{\partial \mathbf{B}}{\partial t}=\nabla\times(\mathbf{V}\times\mathbf{B})+\frac{1}{P_m}\nabla^2\mathbf{B}\,, \qquad (2)$$

$$\frac{\partial T}{\partial t}+(\mathbf{V}\cdot\nabla)\,T=\frac{1}{P_r}\nabla^2 T+H\,, \qquad (3)$$

$$\nabla\cdot\mathbf{V}=0, \quad \nabla\cdot\mathbf{B}=0\,. \qquad (4)$$

The radius of the outer sphere L, is the typical length scale, which makes the dimensionless radius $r_o=1$; the inner core radius r_i is, similar to that of the Earth, equal to 0.35. $(r,\,\theta,\,\varphi)$ is the spherical system of coordinates, $\mathbf{1}_z$ is the unit vector. The typical time, t, is measured in the unit of L^2/ν, typical velocity, $\mathbf{V}$, in ν/L, typical magnetic induction, $\mathbf{B}$, in $(\rho\mu\eta\Omega)^{1/2}$, typical temperature, T, in ΔT, and pressure, P, in $\rho\nu^2/L^2$. The dimensionless parameters appearing in Eqs. (1)–(4) are the Prandtl number, $P_r=\nu/\kappa$, the magnetic Prandtl number, $P_m=\nu/\eta$, the Ekman number, $E=\nu/\Omega L^2$ and the modified Rayleigh number $R_a=\alpha g_0\Delta T L/\nu\Omega$, where κ is the thermal diffusivity, ν is the kinematic viscosity, μ is the magnetic permeability, η is the magnetic diffusivity, ρ is the density, α is the coefficient of thermal expansion, ΔT is the drop of temperature through the shell and g_0 is the gravity acceleration at $r=r_o$.

Eqs. (1)–(4) are closed by the non-penetrating and no-slip boundary conditions for the velocity field at the rigid surfaces and fixed temperature boundary conditions. The outer boundary is electrically insulating (the magnetic field on this boundary matches with the appropriate potential field in the exterior which implies no external sources of the field) and the inner boundary is in the first investigated case electrically insulating, while in the second case it is electrically conducting (electrical conductivity of the outer and inner core is considered to be the same).

The last term in Eq. (3), H, constitutes the internal heat sources (it is the

non-dimensional volumetric heat source strength), which enables simulating thermodynamically the various stratification of the spherical shells also in the Boussinesq models. The outer liquid sphere is assumed to be stratified non-uniformly (it is divided into stably and unstably stratified sub-shells) with a constant temperature $T_i = 1$ and $T_o = 0$ at the inner and outer boundaries of the shell, respectively. As given before, we considered the case where 5% of the radial extent of the shell is stably stratified (the upper sub-shell is stably stratified) and 95% unstably (the lower sub-shell is unstably stratified), i.e. $\partial T/\partial r$ changes its sign at $r_m = 0.9675$. This is accomplished if $H = -2.41 P_r^{-1}$. Let us describe why we used this value. The non-uniform stratification is considered due to internal heat sources and in the basic state Eq. (3) gets the form

$$\frac{1}{P_r}\nabla^2 T + H = 0\,. \tag{5}$$

If we solve Eq. (5) considering $T_i = 1$, $T_o = 0$ and $\partial T/\partial r = 0$ at $r = r_m$, we obtain $H = -2.41 P_r^{-1}$. It is necessary to remark that for the uniform stratification $H = 0$.

3. Numerical results

Eqs. (1)–(4) were solved using the MAG dynamo code (*Olson and Glatzmaier, 1995; Olson and Glatzmaier, 1996; Olson et al., 1999; Christensen et al., 2001; Olson and Glatzmaier, 2005; Christensen and Aubert, 2006*). It is a serial version of Gary Glatzmaier's rotating spherical convection/magneto-convection/dynamo code, modified by Ulrich Christensen and Peter Olson. The code solves the non-dimensional Boussinesq equations for time-dependent thermal convection in a rotating spherical shell filled with an electrically conducting fluid. MAG uses toroidal-poloidal decomposition for velocity and magnetic field with explicit time steps. Linear terms are evaluated spectrally (spherical harmonics plus Chebyshev polynomials in radius) and nonlinear terms are evaluated on a spherical grid (for more details, see *Olson and Glatzmaier, 1995; Olson and Glatzmaier, 1996; Olson et al., 1999; Christensen et al., 1999; Christensen et al., 2001; Olson and Glatzmaier, 2005*). The computations were performed on the Nemo cluster (SGI)

at the Institute of Geophysics, Academy of Sciences of CR, Prague.

Dependence of solutions on various values of the Prandtl number, P_r, the type of density stratification and electromagnetic boundary conditions for given Rayleigh number, R_a, magnetic Prandtl number, P_m and Ekman number, E, was investigated. Computations started from zero initial velocity and strong dipole-dominated field with $B \sim \mathcal{O}(\infty)$, and were performed for $P_r = 0.2, 1, 5$, $E = 10^{-3}$, $P_m = 25$, and $R_a = 120$. In the case of non-uniform stratification $H = -12.05, -2.41, -0.49$ for $P_r = 0.2, 1, 5$, respectively, and in the case of uniform one $H = 0$ (in this case the whole shell is unstably stratified).

At $P_r = 0.2$ the characteristic viscous diffusion time is five times greater than the characteristic thermal diffusion time ($\tau_\nu = 5\tau_\kappa$), i.e. thermal diffusion processes dominate over viscous ones. At $P_r = 1$ the characteristic thermal diffusion time is equal to the characteristic viscous diffusion time ($\tau_\kappa = \tau_\nu$), i.e. thermal and viscous diffusion processes equally affect the dynamics of convection and dynamo. At $P_r = 5$ the characteristic viscous diffusion time is five times smaller than the characteristic thermal diffusion time ($\tau_\kappa = 5\tau_\nu$); i.e. viscous diffusion processes dominate over thermal ones. Dependences of the mean kinetic energy, E_k, and the mean magnetic energy, E_m, on P_r, the type of stratification (uniform and non-uniform) and electromagnetic boundary conditions are given in Table 1. E_k strongly increases for given E, R_a and P_m with decreasing of P_r. Convection is at $P_r = 0.2$ more overcritical than at $P_r = 1$ and $P_r = 5$ and also the convection at $P_r = 1$ is more overcritical than at $P_r = 5$. The critical Rayleigh number, R_{a_c}, decreases with decreasing of P_r, which leads to the convection being more overcritical with decrease of P_r (see *Busse and Simitev, 2005* and Table 1). In Table 1 the values of E_k increase with decreasing of P_r. At $P_r = 0.2$ the kinetic energy is greater in the case of uniform stratification than in the case of non-uniform one, while at $P_r = 1$ and $P_r = 5$ kinetic energies are greater in the case of non-uniform stratification than in the case of uniform one. Thus, at $P_r = 0.2$ the stably stratified sub-shell has a stabilizing influence to the convection (convection is in the case of non-uniform stratification less overcritical than in the case of uniform one), while at $P_r = 1$ and $P_r = 5$ it has a destabilizing influence to the convection (convection is in the case of non-uniform stratification more overcritical than in the case of uniform one, see Table 1). E_m also strongly increases

Table 1. Dependences of the mean kinetic energy, E_k, and the mean magnetic energy, E_m, on P_r, the type of stratification (uniform – UNI and non-uniform – NON-UNI), and electromagnetic boundary conditions (0 – ICB is electrically insulating and 1 – ICB is electrically conducting)

	E_k	E_m
$P_r = 0.2$ UNI 0	936.11	6081.22
$P_r = 0.2$ UNI 1	939.03	6085.69
$P_r = 0.2$ NON-UNI 0	732.18	4968.25
$P_r = 0.2$ NON-UNI 1	734.75	4972.55
$P_r = 1$ UNI 0	32.31	832.34
$P_r = 1$ UNI 1	34.81	839.17
$P_r = 1$ NON-UNI 0	43.56	781.28
$P_r = 1$ NON-UNI 1	45.91	785.35
$P_r = 5$ UNI 0	1.81	153.37
$P_r = 5$ UNI 1	1.84	158.13
$P_r = 5$ NON-UNI 0	1.88	135.09
$P_r = 5$ NON-UNI 1	1.91	136.18

for given E, R_a and P_m with decreasing of P_r. At $P_r = 0.2$ the magnetic energy is greater in the case of uniform stratification than in the case of non-uniform one, while at $P_r = 1$ and $P_r = 5$ magnetic energies are greater in the case of non-uniform stratification than in the case of uniform one (see Table 1). Thus, E_k and E_m strongly depend on the stratification and P_r. However, they are completely independent of the electromagnetic boundary conditions, i.e. electrical conductivity of ICB. In Table 1 the values of E_k and E_m are almost the same for both the ICB to be electrically insulating and electrically conducting.

The typical space distributions of the radial magnetic field component, B_r are presented in Fig. 1, the radial velocity field component, V_r in Fig. 2, the Z-vorticity in Fig. 3 (equatorial sections), the azimuthal magnetic field component, B_φ in Fig. 4 (axi-symmetrical meridional sections) and the azimuthal velocity field component, V_φ in Fig. 5 (axi-symmetrical meridional sections). Finally, the typical space distributions of the radial magnetic field component, B_r at CMB are presented in Fig. 6 and 7. All the figures are snapshots done at time $t = 10$ (10 time units). Figs. (1-2) were done using the value of $r = 0.85$ which lies in the unstable region. However, Figs. (6-7)

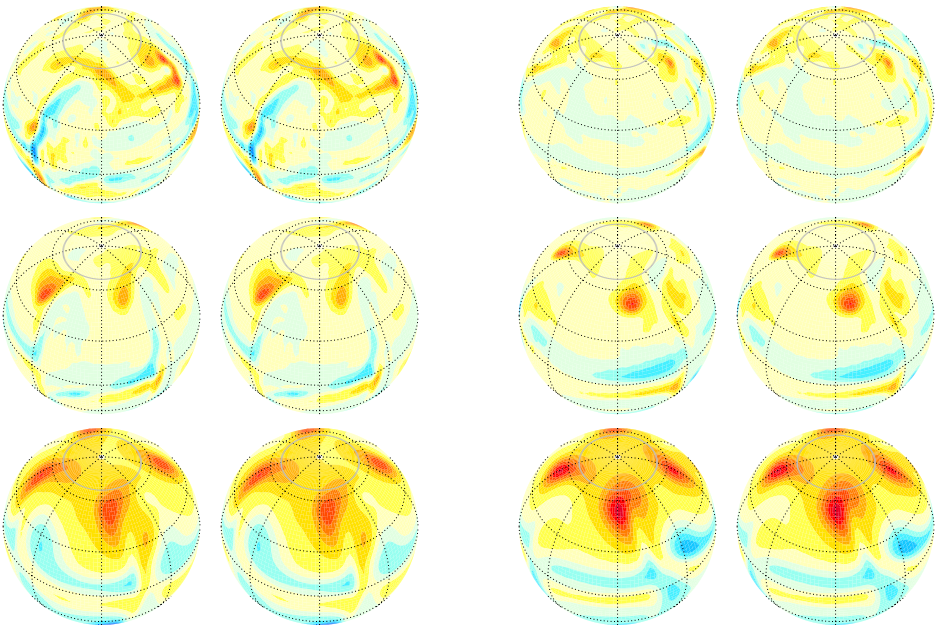

Fig. 1. Space distributions of radial magnetic field components B_r at $r = 0.85$ for $P_r = 0.2$, 1, 5 (from the top to the bottom), for the cases of uniform (left pair in each row) and non-uniform (right pair in each row) stratification, and for ICB to be electrically insulating (left in each pair), ICB to be electrically conducting (right in each pair), $R_a = 120$, $E = 10^{-3}$ and $P_m = 25$. Red (blue) colours indicate positive (negative) values. Snapshots at $t = 10$.

were done using $r = r_o$ (at CMB).

The generated magnetic field is dipolar in all investigated cases. Decreasing P_r we observe breaking of the equatorial antisymmetry (see Figs. 1, 6 and 7). At $P_r = 0.2$ some remnants of equatorial antisymmetry are observed in the case of uniform stratification, while in the case of non-uniform one, it is lost. At $P_r = 1$ and 5 it is possible to observe the equatorial antisymmetry in both types of stratification. At $P_r = 5$ we observe the four-fold symmetry even though it was not prescribed as in *Šimkanin and Hejda (2011)*. In the present study we suppose the full sphere (no symmetry in the azimuthal direction). Magnetic field morphology is slightly influenced by stratification because stably stratified sub-shell is too thin. The generated magnetic fields do not weaken as those in *Šimkanin et al.*

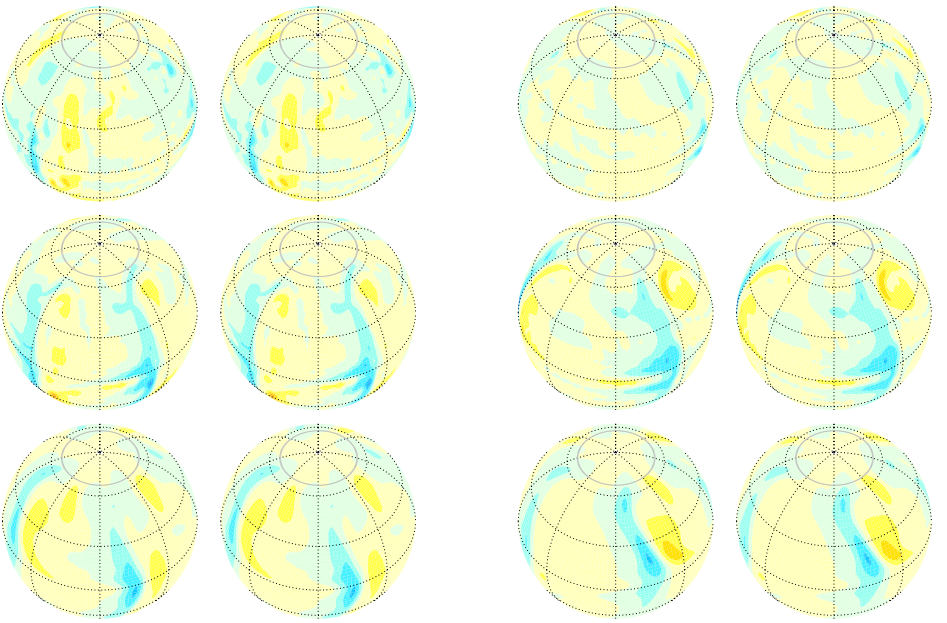

Fig. 2. Space distributions of radial velocity field components V_r at $r = 0.85$ for $P_r = 0.2, 1, 5$ (from the top to the bottom), for the cases of uniform (left pair in each row) and non-uniform (right pair in each row) stratification, and for ICB to be electrically insulating (left in each pair), ICB to be electrically conducting (right in each pair), $R_a = 120$, $E = 10^{-3}$ and $P_m = 25$. Yellow (blue) colours indicate positive (negative) values. Snapshots at $t = 10$.

(2011), where magnetic fields become weak with an increase of the thickness of a stably stratified sub-shell because the stably stratified sublayer acts to destabilize the dynamo (*Stanley and Mohammadi, 2008; Šimkanin et al., 2011*), due to a thin stably stratified sub-shell. The value of P_m was set to 25 to compare dynamos at all the investigated values of P_r. Small P_m is not enough to sustain dynamos at higher values of P_r (e.g., $P_r = 5$). As our $P_m \gg P_{m_c}$ (P_{m_c} is the critical value of P_m, for more details, see *Christensen and Aubert (2006)* and *Šimkanin and Hejda (2011)*, magnetic fields do not become weak in the polar regions (see Fig. 1, 6 and 7) as it was in *Šimkanin and Hejda (2011)* because the magnetic field inside the tangent cylinder is always regenerated (see Fig. 4). The independence of generated magnetic fields on electromagnetic boudary conditions (electrical

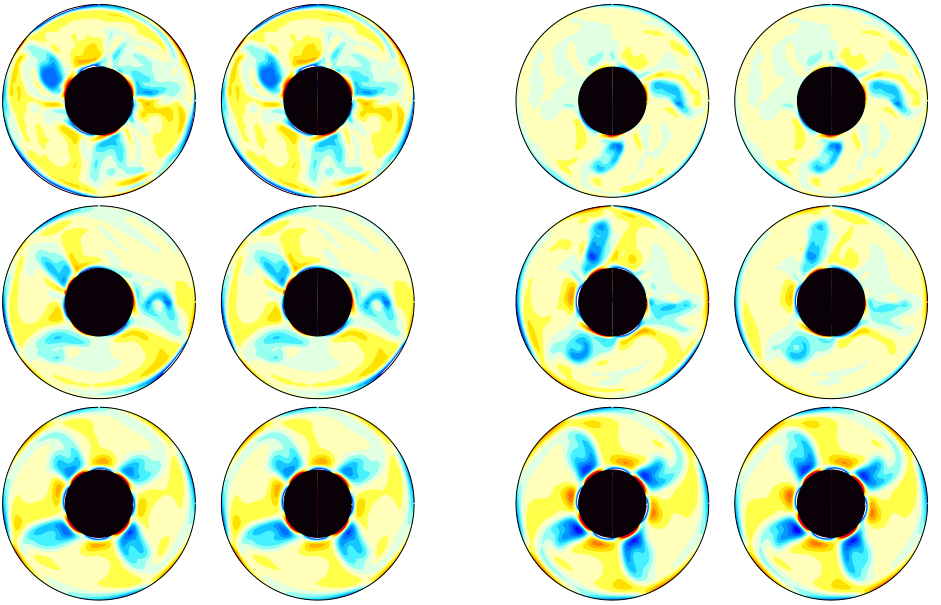

Fig. 3. Equatorial sections of Z-vorticity for $P_r = 0.2$, 1, 5 (from the top to the bottom), for the cases of uniform (left pair in each row) and non-uniform (right pair in each row) stratification, and for ICB to be electrically insulating (left in each pair), ICB to be electrically conducting (right in each pair), $R_a = 120$, $E = 10^{-3}$ and $P_m = 25$. Red (blue) colours indicate positive (negative) values. Snapshots at $t = 10$.

conductivity of ICB) is evident also in Figs. 1, 6 and 7.

Fig. 2 shows the effect of stratification and P_r on radial velocity. The symmetric character of the velocity field about the equator and the spiralling cross section of the columns are typical features for both cases of stratification at $P_r = 1$ and $P_r = 5$. However, at $P_r = 0.2$ the velocity field loses some of its equatorial symmetry (see Fig. 2), while the magnetic field loses its strong antisymmetric character (see Fig. 1). It is typical for low P_r dynamos that the Lorentz forces become weak and the braking of the differential rotation by the Lorentz force is an important effect (*Busse and Simitev, 2005*). However, such an effect is not observed in our case because $P_m \gg P_{m_c}$. In the case of uniform stratification, a large-scale columnar convection is developed in the whole volume, while in the case of non-uniform stratification it is slightly shifted out of CMB (slightly suppressed to the

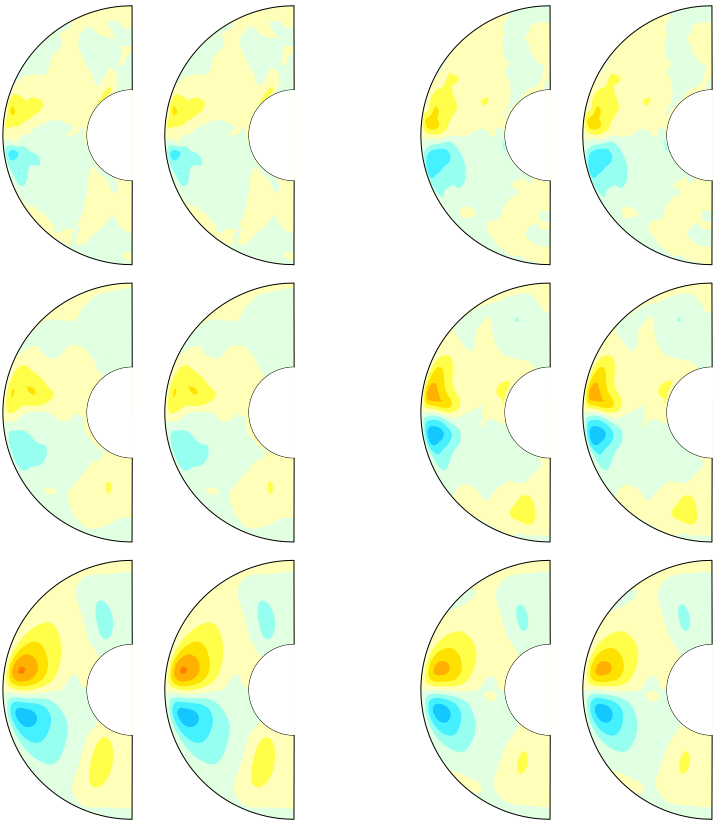

Fig. 4. Axi-symmetrical meridional sections of azimuthal magnetic field components B_φ for $P_r = 0.2, 1, 5$ (from the top to the bottom), for the cases of uniform (left pair in each row) and non-uniform (right pair in each row) stratification, and for ICB to be electrically insulating (left in each pair), ICB to be electrically conducting (right in each pair), $R_a = 120$, $E = 10^{-3}$ and $P_m = 25$. Red (blue) colours indicate positive (negative) values. Snapshots at $t = 10$.

unstably stratified region) but penetrates to the stably stratified one. A measure of such a penetration is governed by the value of the Brunt-Väisälä frequency (e.g. *Takehiro and Lister, 2001; Takehiro and Lister, 2002*). From this point of view a stratified layer acts as a filter of the convection. It is possible to observe in the stably stratified sub-shell a weak tendency of flow to be more toroidal. The radial stratification causes the toroidal motions

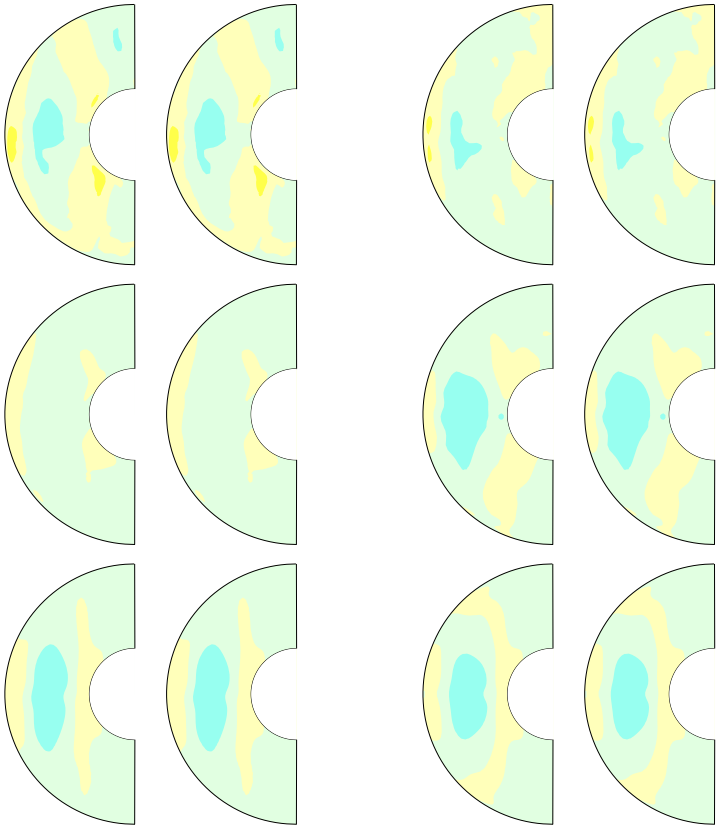

Fig. 5. Axi-symmetrical meridional sections of azimuthal velocity field components V_φ for $P_r = 0.2, 1, 5$ (from the top to the bottom), for the cases of uniform (left pair in each row) and non-uniform (right pair in each row) stratification, and for ICB to be electrically insulating (left in each pair), ICB to be electrically conducting (right in each pair), $R_a = 120$, $E = 10^{-3}$ and $P_m = 25$. Yellow (blue) colours indicate positive (negative) values. Snapshots at $t = 10$.

in the outermost part of the shell (teleconvection). It cannot take place without such a radial stratification and is possible if the unstable stratification dominates over the stable one (*Zhang and Schubert, 2000; Busse and Simitev, 2005; Šimkanin et al., 2010; Šimkanin et al., 2011*). The multilayer convection (teleconvection) is not developed in our case. This is a little strange because the stably stratified sub-shell is thin (the unstable

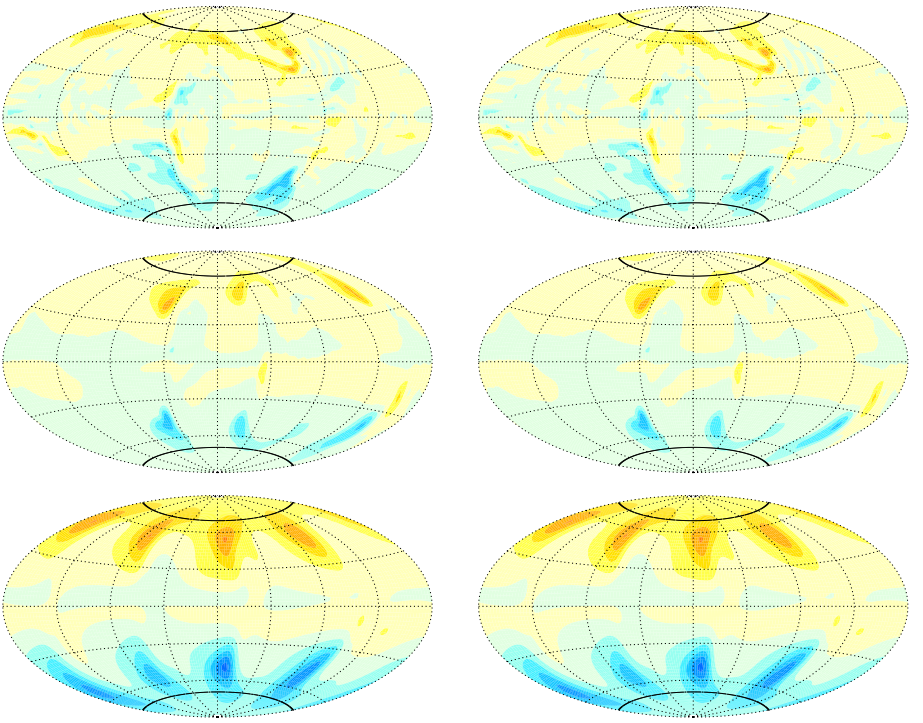

Fig. 6. Space distributions of radial magnetic field components B_r at $r = r_o$ for $P_r = 0.2, 1, 5$ (from the top to the bottom), for ICB to be electrically insulating (left column) and ICB to be electrically conducting (right column), in the case of uniform stratification, and for $R_a = 120$, $E = 10^{-3}$ and $P_m = 25$. Red (blue) colours indicate positive (negative) values. Snapshots at $t = 10$.

stratification dominates over the stable one) and for the same amount of stably stratified sub-shell *Šimkanin et al. (2011)* observed the multilayer convection. The velocity V_r is also more concentrated into the structure with larger scale in the case of high value of P_r, where it is possible to see more columnar shape at $P_r = 5$ than at $P_r = 0.2$. However, the columnarity at high P_r is not so obvious than in the case of B_r in Fig. 1.

One can observe similar behaviour for azimuthal components of velocity (Fig. 5) and magnetic field (Fig. 4). V_φ is at high P_r more columnar and the effect of inner core and tangent cylinder is more visible. B_φ is concentrated into azimuthal structures. The separation of the azimuthal velocity

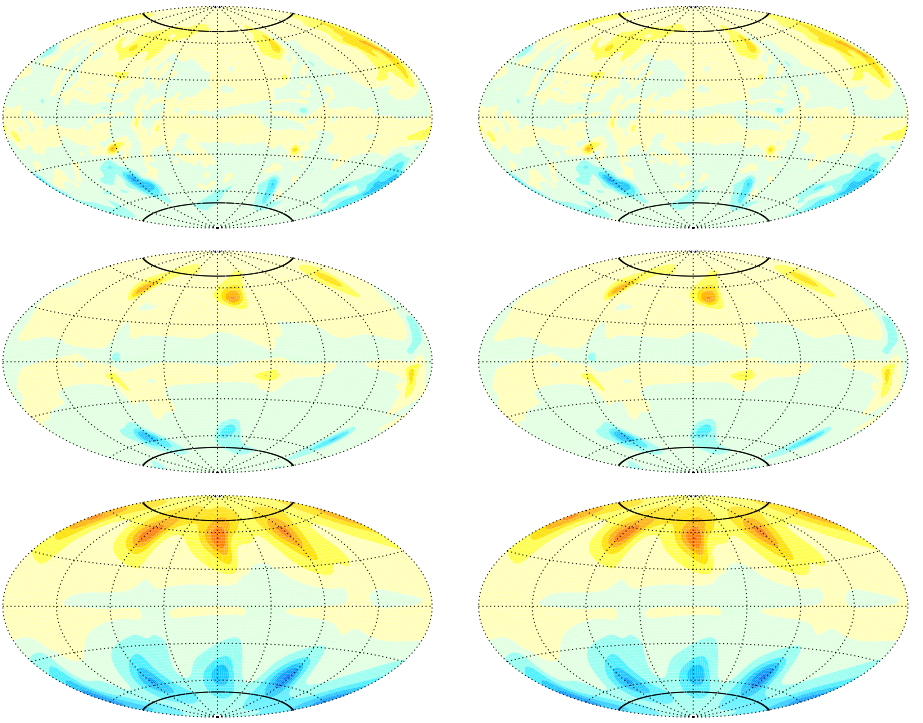

Fig. 7. The same as in Fig. 6 but in the case of non-uniform stratification.

to the regions inside the tangent cylinder and outside the tangent cylinder is weakened. Especially in the case of $P_r = 5$ (see Fig. 5, bottom) one can see obvious structures aligned with the rotation axis in the case of uniform stratification (left) but slightly disturbed in the case of non-uniform stratification (right). A sharp border as a consequence of the tangent cylinder is not present in the azimuthal magnetic field in Fig. 4. Magnetic field (unlike velocity field) is controled by Coriolis force only indirectly due to the frozen magnetic fieldlines.

4. Discussion

Density stratification, diffusive processes and electomagnetic properties of boundaries play a significant role in geophysical processes (e.g. *Braginsky,*

1964; Fearn and Loper, 1981; Christensen, 2006; Christensen and Wicht, 2008; Stanley and Bloxham, 2004; Stanley and Bloxham, 2006; Wicht, 2002; Stanley and Mohammadi, 2008; Zhang, 1994; Zhang and Schubert, 2000; Šimkanin et al., 2003; Šimkanin et al., 2006; Šimkanin et al., 2010). We present a study of the simultaneous influence of the non-uniform stratification, electrical conductivity of the inner core and diffusive processes on the dynamo action. Our results show that the dynamo action, especially the magnetic field structure, is independent in our investigated cases of the electrical conductivity of the inner core. This result strongly supports results provided in *Wicht (2002)*, where the influence of the inner-core conductivity on the field structure in the outer core and on Earth-like reversal sequences was found to be insignificant.

The influence of non-uniform stratification is weak for our parameters. This is understandable because most of the shell is unstably stratified, and the stably stratified region is only a thin layer near the CMB. This type of stratification has a weak effect on the dynamo. The magnetic field at CMB is in the case of non-uniform stratification a little weaker than in the uniform case (see Figs. 6 and 7) but this difference is almost negligible. However, *Stanley and Mohammadi (2008)* and *Gubbins and Davies (2013)* showed stronger influence of a thin stable layer near the CMB on convection and dynamo action. *Stanley and Mohammadi (2008)* showed that a thin stable layer in the dynamo models acts to destabilize the dynamo and the drift of magnetic flux spots in the equatorial regions is eastwards. However, the geomagnetic observations show a westward drift, their models then suggest that the Earth's core does not contain a stable layer (*Stanley and Mohammadi, 2008*). Our results show that the thin stably stratified subshell very slightly destabilize the dynamo at all the investigated values of P_r (magnetic fields are weaker in the case of non-uniform stratification). We do not observe in our dynamos an eastward drift of magnetic flux spots in the equatorial regions; it is always westwards. Probably, our stably stratified layer is not very strongly stratified. The magnitude of the subadiabatic stratification is similar to that of the superadiabatic stratification. It is possible that the stable layer near the CMB could be very strongly stratified but our model is perhaps characterized by the mild stable stratification. *Stanley and Mohammadi (2008)* and *Gubbins and Davies (2013)* likely used a stronger stratification than us, which might account for the difference. Thus, our

results support the ones provided in *Šimkanin et al. (2010), Šimkanin et al. (2011), Šimkanin and Hejda (2011)* although the teleconvection is not observed in our study.

The influence of the Prandtl number is strong. Convection is at $P_r = 0.2$ most overcritical, more than at $P_r = 1$ and $P_r = 1$ is more overcritical than at $P_r = 5$. So, the generated magnetic field is the strongest one at $P_r = 0.2$, while at $P_r = 5$ it is the weakest one (see Table 1). Our magnetic fields do not become weak in the polar regions as it was in *Šimkanin and Hejda (2011)* because the magnetic field inside the tangent cylinder is always regenerated due to the weak magnetic diffusion (see Figs. 1, 4, 6 and 7). This is because we set $P_m \gg P_{m_c}$ and at these values of P_m magnetic fields never become weak in polar regions (as shown in *Šimkanin and Hejda, 2011*). Consequently, our dynamos are dependent mostly on the Prandtl number.

Acknowledgments. This study was supported by the Ministry of Education, Youth and Sports through project No. LG13042 and by the Scientific Grant Agency VEGA through project No. 1/0523/13. We would like to thank G. Glatzmaier, U. Christensen, P. Olson and CIG for the MAG dynamo code, and the Institute of Geophysics, Academy of Sciences of the CR, Prague for CPU time on the NEMO cluster (SGI).

References

Bassom A. P., Soward A. M., Starchenko S. V., 2011: The onset of strongly localized thermal convection in rotating spherical shells. J. Fluid Mech., **689**, 376–416, doi: 10.1017/jfm.2011.421.

Braginsky S., 1964: Magnetohydrodynamics of the Earth's Core. Geomagn. Aeron., **4**, 898–916 (Engl. Transl. 698–712).

Busse F. H., Simitev R., 2005: Convection in rotating spherical fluid shells and its dynamo states. In: Fluid Dynamics and Dynamos in Astrophysics and Geophysics, pp. 359–392, Eds. Soward A. M., Jones C. A., Hughes D. W., Weiss N. O., CRC Press, New York, USA.

Christensen U. R., 2006: A deep dynamo generating Mercury's magnetic field. Nature, **444**, 1056–1058, doi: 10.1038/nature05342.

Christensen U. R., Aubert J., 2006: Scaling properties of convection driven dynamos in rotating spherical shells and application to planetary magnetic fields. Geophys. J. Int., **166**, 97–114.

Christensen U. R., Wicht J., 2007: Numerical dynamo simulations. In: Volume 8 – Core Dynamics, pp. 245–282, Ed. Kono M., Treatise on Geophysics, ed. Schubert G., Elsevier, Amsterdam.

Christensen U. R., Wicht J., 2008: Models of magnetic field generation in partly stable planetary cores: applications to Mercury and Saturn. Icarus, **196**, 16–34.

Christensen U. R., Aubert J., Cardin P., Dormy E., Gibbons S., Glatzmaier G. A., Grote E., Honkura Y., Jones C., Kono M., Matsushima M., Sakuraba A., Takahashi F., Tilgner A., Wicht J., Zhang K., 2001: A numerical dynamo benchmark. Phys. Earth Planet. Inter., **128**, 25–34.

Dharmaraj G., Stanley S., 2012: Effect of inner core conductivity on planetary dynamo models. Phys. Earth Planet. Inter., **212–213**, 1–9.

Fearn D. R., Roberts P. H., 2007: 4.1. The Earth and its magnetic field, in Mathematical Aspects of Natural Dynamos, pp. 201–209, Ed. Soward A. M., Dormy E., CRC Press, New York, USA.

Fearn D. R., Loper D. E., 1981: Compositional convection and stratification of the Earth's core. Nature, **289**, 393–394.

Glatzmaier G. A., 2005: Planetary and stellar dynamos: challenges for next generation models. In: Fluid Dynamics and Dynamos in Astrophysics and Geophysics, pp. 331–357, Eds Soward A. M., Jones C. A., Hughes D. W., Weiss N. O., CRC Press, New York, USA.

Gubbins D., Davies C. J., 2013: The stratified layer at the core-mantle boundary caused by barodiffusion of oxygen, sulphur and silicon. Phys. Earth Planet Inter., **215**, 21–28.

Jones C. A., 2000: Convection-driven geodynamo models. Phil. Trans. R. Soc. Lond., **A358**, 873–897.

Olson P., Glatzmaier G. A., 1995: Magnetoconvection in a rotating spherical shell: structure of flow in the outer core. Phys. Earth Planet Inter., **92**, 109–118.

Olson P., Glatzmaier G. A., 1996: Magnetoconvection and thermal coupling of the Earth's core and mantle. Phil. Trans. R. Soc. Lond., **A354**, 1413–1424.

Olson P., Glatzmaier G. A., 2005: Probing the geodynamo. Scientific American, **15**, 2, 29–35.

Olson P., Christensen U. R., Glatzmaier G. A., 1999: Numerical modeling of the geodynamo: mechanisms of field generation and equilibration. J. Geophys. Res., **104**, 10, 383–404.

Roberts P. H., Glatzmaier G. A., 2000: Geodynamo theory and simulations. Rev. Mod. Phys., **72**, 4, 1081–1123.

Sakuraba A., Roberts P. H., 2009: Generation of a strong magnetic field using uniform heat flux at the surface of the core. Nature Geosci., **2**, 802–805.

Stanley S., Bloxham J., 2004: Convective-region geometry as the cause of Uranus' and Neptune's unusual magnetic fields. Nature, **428**, 151–153.

Stanley S., Bloxham J., 2006: Numerical dynamo models of Uranus' and Neptune's magnetic fields. Icarus, **184**, 556–572.

Stanley S., Mohammadi A., 2008: Effects of an outer thin stably stratified layer on planetary dynamos. Phys. Earth Planet. Inter., **168**, 179–190.

Šimkanin J., Hejda P., 2011: Hydromagnetic dynamos in rotating spherical fluid shells in dependence on the Prandtl number and stratification. Geophys. J. Int., **185**, 637–646.

Šimkanin J., Brestenský J., Ševčík S., 2003: Problem of the rotating magnetoconvection in variously stratified fluid layer revisited. Studia Geophys. Geod., **47**, 4, 827–845.

Šimkanin J., Brestenský J., Ševčík, S., 2006: On hydromagnetic instabilities and the mean electromotive force in a non-uniformly stratified Earth's core affected by viscosity. Stud. Geophys. Geod., **50**, 645–661.

Šimkanin J., Hejda P., Saxonbergová-Jankovičová D., 2010: Convection in rotating non-uniformly stratified spherical fluid shells in dependence on Ekman and Prandtl numbers. Phys. Earth Planet. Inter., **178**, 39–47.

Šimkanin J., Hejda P., Saxonbergová D., 2011: Hydromagnetic dynamos in rotating non-uniformly stratified spherical fluid shells in dependence on the Rayleigh number. Phys. Earth Planet. Inter., **185**, 100–106.

Takehiro S., Lister J. R., 2001: Penetration of columnar convection into an outer stably stratified layer in rapidly rotating spherical fluid shells. Earth Planet. Sci. Lett., **187**, 357–366.

Takehiro S., Lister J. R., 2002: Surface zonal flows induced by thermal convection trapped below a stably stratified layer in a rapidly rotating spherical shell. Geophys. Res. Lett., **29**, 16, 50-1–50-4.

Trümper T., Breuer M., Hansen U., 2012: Numerical study on double-diffusive convection in the Earth's core. Phys. Earth Planet. Int., **194**, 55–63.

Wicht J., 2002: Inner-core conductivity in numerical dynamo simulations. Phys. Earth Planet. Inter., **132**, 281–302.

Wicht J., Tilgner A., 2010: Theory and modeling of planetary dynamos. Space Sci. Rev., **152**, 501–542.

Zhang K., 1994: On coupling between the Poincare equation and the heat-equation. J. Fluid Mech., **268**, 211–229.

Zhang K., Schubert G., 2000: Teleconvection: remotely driven thermal convection in rotating stratified spherical layers, Science, **290**, 1944–1947.